

Pressure-induced superconductivity and Mott transition in spin-liquid κ -(ET)₂Cu₂(CN)₃ probed by ¹³C NMR

Y. Shimizu,^{1,2,*} H. Kasahara,¹ T. Furuta,¹ K. Miyagawa,¹ K. Kanoda,¹ M. Maesato,² and G. Saito^{2,†}¹Department of Applied Physics, University of Tokyo, Bunkyo-ku, Tokyo 113-8656, Japan²Division of Chemistry, Kyoto University, Sakyo-ku, Kyoto 606-8502, Japan

(Received 29 November 2009; revised manuscript received 13 May 2010; published 9 June 2010)

Pressure-induced superconductivity and Mott transition in the spin-liquid Mott insulator κ -(ET)₂Cu₂(CN)₃ have been investigated by ¹³C NMR measurements. The Mott transition from the spin liquid to the Fermi liquid is observed as a sudden decrease in $1/T_1T$, where T_1 is the nuclear-spin-lattice relaxation time. Pseudogap behavior is absent in the Fermi-liquid state, unlike in the metallic phase adjacent to the antiferromagnetic Mott insulator. In the superconducting state, $1/T_1$ have a cubic temperature dependence with no Hebel-Slichter peak, which is consistent with non-*s*-wave superconducting pairing.

DOI: [10.1103/PhysRevB.81.224508](https://doi.org/10.1103/PhysRevB.81.224508)

PACS number(s): 74.20.Rp, 74.25.N-, 74.70.Kn, 71.30.+h

I. INTRODUCTION

Superconductivity in correlated electron systems usually appears near the long-range magnetic order, as observed in the copper oxide superconductors¹ and heavy-fermion systems.² On the other hand, the superconductivity emerging from a quantum spin liquid has been sought since the proposal of a resonating valence bond state by Anderson.³ The candidates have been geometrically frustrated systems, including triangular lattices, in which the superconducting pairing is theoretically nontrivial because of the depressed magnetic correlation and the absence of the electron scattering at preferential wave vectors on the circular Fermi surface.⁴

One model material is the layered organic superconductor κ -(ET)₂X, which has a half-filled triangular lattice. In the distorted triangular lattice, the ground state of the Mott insulator has antiferromagnetic long-range order, as observed in κ -(d8-ET)₂Cu[N(CN)₂]Br [d8 denotes the full deuteration of ET] and κ -(ET)₂Cu[N(CN)₂]Cl. These materials have a Mott transition at low temperatures and a superconducting transition at $T_c \sim 13$ K under pressure.⁵ For the ambient-pressure superconductor κ -(ET)₂Cu[N(CN)₂]Br, the superconducting order parameter is likely a spin-singlet *d* wave or an anisotropic *s* wave, according to the majority of experiments.⁶ Near the Mott boundary, the normal metallic state exhibits the pseudogapped behavior in the ¹³C nuclear-spin-lattice relaxation rate $1/T_1$, demonstrating a possible precursor of superconductivity.⁷ In clear contrast, another Mott insulator κ -(ET)₂Cu₂(CN)₃, which has a more triangular lattice, exhibits no long-range magnetic order down to 20 mK despite an antiferromagnetic exchange interaction $J \sim 250$ K.^{8,9} The power-law temperature (*T*) dependence of $1/T_1$ at low temperatures is indicative of low-lying spin excitations.⁹ A finite residual density of states has been observed by a specific-heat measurement,¹⁰ whereas thermal-conductivity measurements support the opening of a spin gap.¹¹ The presence or absence of a spinon Fermi surface is currently under active debate.^{12–16}

Besides the nature of the spin-liquid state, the superconducting and metallic states emerging across the Mott transition are not well understood, since the only known example

is κ -(ET)₂Cu₂(CN)₃. In a pressure-temperature phase diagram based on resistivity and ¹H NMR studies, a superconducting phase ($T_c \sim 4$ K) abuts the spin-liquid phase.¹⁷ The slope of the first-order Mott transition line in the phase diagram remains positive down to low temperatures,¹⁷ in contrast to the behavior of κ -(ET)₂Cu[N(CN)₂]Cl.¹⁸ This implies a larger spin entropy in the spin-liquid state than in the neighboring Fermi liquid. The superconducting pairing symmetry in κ -(ET)₂Cu₂(CN)₃ has been extensively theoretically investigated.^{19–30} The suppression of spin fluctuations diminishes superconductivity in a regular triangular lattice but the $d_{x^2-y^2}$ pairing becomes favorable when the lattice is distorted.^{19–22} Even if a superconducting state appears, $d_{x^2-y^2}$, $d_{x^2-y^2} + id_{xy}$, $d_{x^2-y^2} + is$, or *p*-wave pairings are proposed for the triangular lattice.^{23–28} An exotic superconducting state due to Amperian or triplet pairing may emerge from the spin liquid.^{29,30}

The previous ¹H NMR study under pressure could not detect a superconducting state because the random orientation of the polycrystalline sample suppressed the upper critical field H_{c2} .¹⁷ Even in a superconducting state, ¹H NMR is usually susceptible to vortex dynamics in layered superconductors.³¹ In this paper, we report ¹³C NMR measurements of a ¹³C-enriched single crystal of κ -(ET)₂Cu₂(CN)₃ under hydrostatic pressure. A large hyperfine coupling at ¹³C sites and a precise alignment of the magnetic field allowed us to observe quasiparticle excitations of the superconducting state. We observed the T^3 behavior of $1/T_1$ in the superconducting state, as expected for an anisotropic order parameter, and analogous to the other κ -(ET)₂X members, whereas the Knight shift underwent a small but finite decrease. The dynamic and static spin susceptibilities in the normal metallic state are also presented.

II. EXPERIMENTAL

To conduct ¹³C NMR measurements of κ -(ET)₂Cu₂(CN)₃, the double-bonded carbon sites at the center of the ET were selectively enriched with ¹³C isotope to 98% concentration.³² A single crystal 1 mm × 1.5 mm × 0.05 mm in size was soaked into a pressure medium of

Daphne 7373 and placed in a BeCu pressure cell. A pressure of 0.4 GPa was applied at room temperature, slightly exceeding the critical pressure of the Mott transition.¹⁷ The pressure cell was uniaxially rotated in the magnetic field with a precision of 0.1° . The spin-echo signal was measured using a $\pi/2$ - τ - π pulse sequence under a static magnetic field $H_0 = 2.0$ or 3.5 T parallel to the conducting layer. The typical length of the $\pi/2$ pulse was $1 \mu\text{s}$ and the interval between the $\pi/2$ and π pulses, τ , was $20 \mu\text{s}$ ($\ll T_1$). T_1 was obtained from the saturation recovery of the nuclear magnetization, which was well fitted by the single-exponential function, $1 - M(t)/M(\infty) = \exp(-t/T_1)$, where M is the spin-echo intensity integrated over all ^{13}C resonance lines to provide a sufficient signal-to-noise ratio. The analysis did not qualitatively affect the T dependence of $1/T_1$ since T_1 averaging due to spectral broadening and nuclear-spin-spin relaxation did not allow an independent determination of T_1 of each constituent line. The intensity of the spin-echo signal was much lower than that of the extrinsic ringing signal after the π pulse at the low frequency of 21 MHz. We employed the time spectrum soon after the saturation comb pulses (comb 2 ms $\pi/2$ - τ - π) as a background, which was effective in the present experiments with T_1 of longer than 50 ms. The frequency spectrum was obtained by Fourier transformation of the time spectrum. The ^{13}C Knight shift K was defined as the relative shift from the resonance frequency of the tetramethylsilane reference sample.

III. RESULTS AND DISCUSSION

To probe the superconducting state by NMR, one should align the magnetic field precisely parallel to conducting layer, in order to minimize orbital pair breaking and maximize H_{c2} . In weakly coupled superconducting layers, vortices are locked into the anion layer as Josephson vortices without fluctuations of in-plane pancake vortices, which would cause an additional spin-lattice relaxation.³¹ We determined the parallel-field geometry in the superconducting state by measuring the resonance frequency of the NMR tank circuit, ν_{LC} , at $H_0 = 0.2$ and 2 T. Figure 1(a) shows ν_{LC} plotted against the angle between the magnetic field and the superconducting layer at 1.5 and 10 K, well below and above T_c , respectively. While ν_{LC} is insensitive to the H_0 direction at 10 K, a decrease in ν_{LC} is observed in a narrow angle range ($\sim 0.2^\circ$ bottom width) at 1.5 K. Such a dip structure is expected to appear in a parallel-field geometry [the right panel in Fig. 1(a)].³³

ν_{LC} was measured on cooling the sample at various H_0 parallel to the layers as shown in Fig. 1(b). In the absence of a static magnetic field, the sudden increase in ν_{LC} below 3.8 K signifies a superconducting transition, in good agreement with the resistivity measurement of $T_c = 4$ K.¹⁷ The application of a magnetic field lowers T_c and reduces the ν_{LC} increase due to easier penetration of vortices.^{33,34} The H_0 dependence of the onset T_c marked by arrows in Fig. 1(b) gives the T - H_{c2} diagram for the in-plane magnetic field as shown in the inset. An extrapolation of H_{c2} to $T = 0$ yields $H_{c2}(0) = 10$ – 12 T, somewhat exceeding the Pauli limiting field of 7.5 T. NMR measurements were conducted at $H_0 = 2$ T and

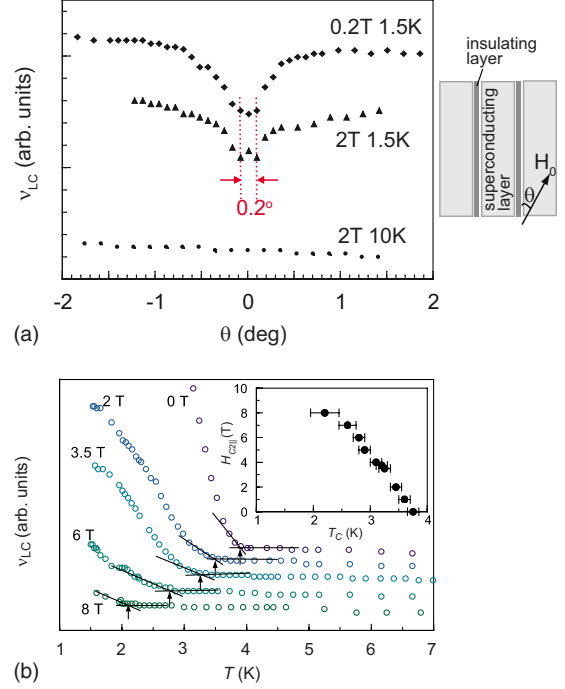


FIG. 1. (Color online) (a) Angular dependence of the resonance frequency of the NMR tank circuit, ν_{LC} , and a schematic configuration of magnetic field. (b) Temperature dependence of ν_{LC} at various magnetic fields parallel to the layer. Inset: H_{c2} vs T_c , as indicated by the arrows in the main figure.

3.5 T, where $T_c = 3.5$ K and 3.3 K, respectively.

Figure 2 shows the T dependence of ^{13}C NMR spectra measured at $H_0 = 3.5$ T ($T_c = 3.3$ K). There are four inequivalent ^{13}C sites: two ET (labeled A and B in the right panel of Fig. 2) are inequivalent against the applied field and each ET contains two inequivalent ^{13}C (labeled 1 and 2 with

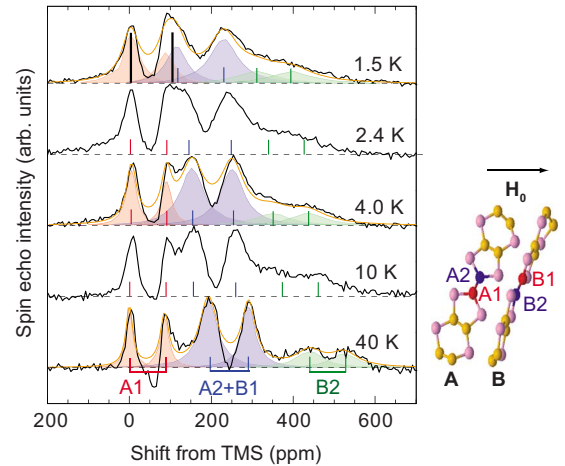


FIG. 2. (Color online) ^{13}C NMR spectra at 0.4 GPa with $H_0 = 3.5$ T parallel to the conducting layer. The colored vertical lines are the centers of the fitting spectra (the shaded spectra and solid lines are the fit for each line and the sum, respectively). Bold vertical lines indicate the $\chi_{\text{spin}} = 0$ positions evaluated from the K - χ_{spin} plots in Fig. 3. Right figure: corresponding ^{13}C sites in ET molecules.

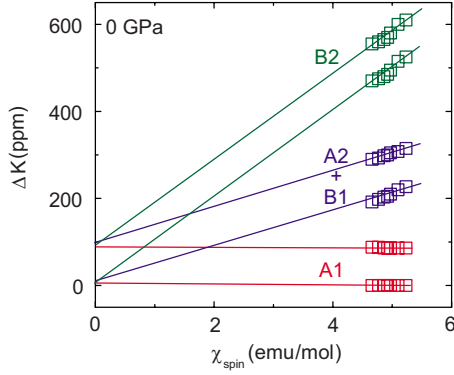


FIG. 3. (Color online) K vs χ_{spin} plots for three ^{13}C sites, defined in Fig. 2, at ambient pressure. The magnetic field was applied in the same direction as in the experiments at 0.4 GPa.

different hyperfine couplings to electron spin. Each line splits into a doublet due to nuclear dipole-dipole interaction (Pake doublet), resulting in a total of eight lines. We observed three doublets in the 40 K spectrum and the intensity of the middle doublet was twice as high as those of the other doublets because of accidental superposition of the A2 and B1 lines.

As T is lowered from 40 to 10 K, the A2+B1 and B2 lines shift appreciably toward lower frequencies, reflecting the T dependence of the spin susceptibility χ_{spin} in the normal state. Below 10 K, the spectra broadened, making the definition of K ambiguous. We defined K by fitting the spectra to a superposition of six Lorentzians (colored solid and dotted lines in Fig. 2) with minimum parameters, assuming that the spectral weights and nuclear dipole splitting are independent of T . Spectrum analysis indicates that K decreases for A2+B1 and B2 but slightly increases for A1, as shown in Fig. 2. Therefore, the hyperfine coupling constant A_{hf} increases in the order: A1, A2+B1, and B2.

Since the orbital contributions to K are negligible in organic conductors that have well-separated orbital energy levels and negligible spin-orbit coupling, K can be expressed as $K = A_{\text{hf}}\chi_{\text{spin}}/N\mu_B + K_0$, where K_0 is the T -invariant component including the chemical shift and the Pake doublet. To evaluate χ_{spin} , we determined A_{hf} for each ^{13}C site from K - χ_{spin} plots at ambient pressure with the same field direction as at 0.4 GPa, as shown in Fig. 3, using the known χ_{spin} values.⁸ We assumed that A_{hf} is nearly independent of pressure, as expected from the small lattice contraction of less than 4% at 1.2 GPa in $\kappa\text{-(ET)}_2\text{Cu(NCS)}_2$,³⁵ and from the absence of symmetry breaking across the Mott transition. The linearity in the K - χ_{spin} plot gives $A_{\text{hf}} = 0.3(\pm 0.03) \text{ T}/\mu_B$ and $0.5(\pm 0.05) \text{ T}/\mu_B$ for A2+B1 and B2, respectively, while the intercept of the vertical axis gives chemical shifts of the Pake doublet of 10 ± 10 and 95 ± 10 ppm, as marked by the bold vertical lines in Fig. 2.

Using A_{hf} , we transformed K at 0.4 GPa into χ_{spin} , as shown in Fig. 4(a). For comparison, χ_{spin} of the Mott insulators $\kappa\text{-(ET)}_2\text{Cu}_2(\text{CN})_3$ and $\kappa\text{-(d8-ET)}_2\text{Cu[N(CN)}_2\text{]Br}$ at ambient pressure are also displayed in Fig. 4(a) with the core diamagnetic susceptibility already subtracted.^{7,8} In the Mott insulating phase at ambient pressure, χ_{spin} of $\kappa\text{-(ET)}_2\text{Cu}_2(\text{CN})_3$ decreases smoothly with T below 50 K,⁸

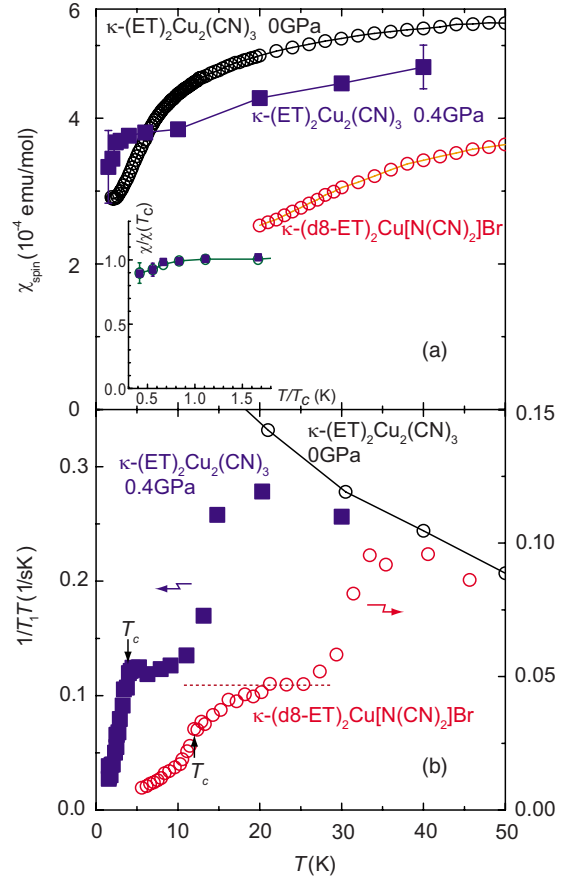


FIG. 4. (Color online) Temperature dependence of (a) spin susceptibility χ_{spin} and (b) $1/T_1T$, for $\kappa\text{-(ET)}_2\text{Cu}_2(\text{CN})_3$ at 0.4 GPa and ambient pressure, and $\kappa\text{-(d8-ET)}_2\text{Cu[N(CN)}_2\text{]Br}$ (Ref. 7). T_1 at ambient pressure was obtained for the A site in a field normal to the layer (Ref. 9). The inset in (a) shows χ_{spin} vs T normalized at T_c .

although the values are much larger than those of $\kappa\text{-(d8-ET)}_2\text{Cu[N(CN)}_2\text{]Br}$, which exhibits macroscopic phase separation below 30 K into an antiferromagnetic insulating phase ($T_N = 18$ K) and a metallic phase. At 0.4 GPa, χ_{spin} of $\kappa\text{-(ET)}_2\text{Cu}_2(\text{CN})_3$ is remarkably insensitive to temperature but continuously decreases across the Mott transition at 10–20 K. Once χ_{spin} becomes constant below 10 K, an appreciable decrease is observed below T_c . While this could be a signature of spin-singlet pairing, the decrease seems insufficient for conventional singlet pairing as shown in the inset of Fig. 4(a). Note that the site-dependent K shown in Fig. 2 rules out the effect of superconducting diamagnetic shielding on the shift below T_c .

One possible reason for the insufficient decrease in K is the presence of triplet Cooper pairing. However, one must consider the rf heating problem that is sometimes encountered in pulse NMR measurements of good conductors at low temperatures. In the superconducting state, the inelastic motion of vortices can produce Joule heating. Although T_1 measurements would be unaffected by this heating due to the long T_1 (> 2 s below 4 K), the spin echo reflects the electronic temperature several tens to hundreds of microsecond after the rf pulses, which is much shorter than T_1 , and therefore could suffer from the heating problem. However, it was

difficult to determine the electronic temperature soon after the rf pulse in the present experimental setup. One method of minimizing rf heating is to measure, instead of the spin echo, the free-induction decay (FID) at low rf power to obtain NMR spectra. Unfortunately, this method was difficult to apply to the present measurements because the extrinsic rf ringing signal obscured the weak FID signals with short T_2^* on the order of several tens of microsecond. By separate experiments, however, we observed the rf power dependence of the shift decrease below T_c in superconducting κ -(ET) $_2$ Cu(NCS) $_2$ under pressure. Thus, the rf heating effect was not ruled out even in the present measurements. Confirmation of the possible mixing of triplet pairing requires further experiments at lower temperatures using lower rf power, which has not yet been accessible due to the small crystal size. Another possible origin for the small change in Knight shift is sample inhomogeneity due to metal-insulator phase separation near the critical pressure of the Mott transition, as observed in κ -(d8-ET) $_2$ Cu[N(CN) $_2$]Br below 30 K. As described below, however, the profile of the nuclear relaxation curve, which would reflect the phase mixture, remained single exponential and unchanged across T_c , indicating no appreciable phase separation.

The T dependence of $1/T_1T$, which measures the wave-vector summation of the dynamical spin susceptibility, is displayed in Fig. 4(b). In the Mott insulating state, $1/T_1T$ increases with decreasing T , indicating the growth of antiferromagnetic correlations. At 0.4 GPa, $1/T_1T$ decreases abruptly at 15 K, where the (first-order) insulator-metal transition was observed in the resistivity.¹⁷ Hence the suppression of magnetic correlation coincides with the Mott transition from a paramagnetic Mott insulator to a metal. Similar behavior was observed in κ -(d8-ET) $_2$ Cu[N(CN) $_2$]Br at 30 K, as also shown in Fig. 4(b).⁷ Once the system gets into the metallic state, the Korringa's relation, $1/T_1T = \text{constant}$, is preserved in the T range between 4 and 10 K. This is in contrast to a depression of $1/T_1T$ in the metallic phase of κ -(d8-ET) $_2$ Cu[N(CN) $_2$]Br below 22 K.⁷ Note that, in the metallic state, the $1/T_1T$ and χ_{spin} values of κ -(ET) $_2$ Cu $_2$ (CN) $_3$ are larger than those of κ -(d8-ET) $_2$ Cu[N(CN) $_2$]Br. This can be attributed to a higher density of states due to strong electron correlations and the absence of a pseudogap. Nevertheless, the superconducting transition temperature of κ -(ET) $_2$ Cu $_2$ (CN) $_3$ is much lower than those of κ -(d8-ET) $_2$ Cu[N(CN) $_2$]Br and κ -(ET) $_2$ Cu[N(CN) $_2$]Cl under pressure. If the pseudogap behavior is related to short-range spin correlation in the neighboring Mott insulating phase, the absence of the pseudogap may arise from frustrated spin correlation in the triangular lattice.

The low-temperature region of $1/T_1$ is shown in Fig. 5, where the upper inset shows the exponent β in the stretched exponential fit, $\exp[-(t/T_1)^\beta]$, to the recovery curve of the nuclear magnetization. β is close to unity and independent of temperature across T_c , which rules out macroscopic phase separation across the first-order Mott transition under the present pressure and magnetic fields. A slight deviation from $\beta=1$ stems from averaging of inequivalent ^{13}C lines with differing T_1 values. With decreasing T , $1/T_1$ decreases linearly at high temperatures, as shown in the lower inset, but

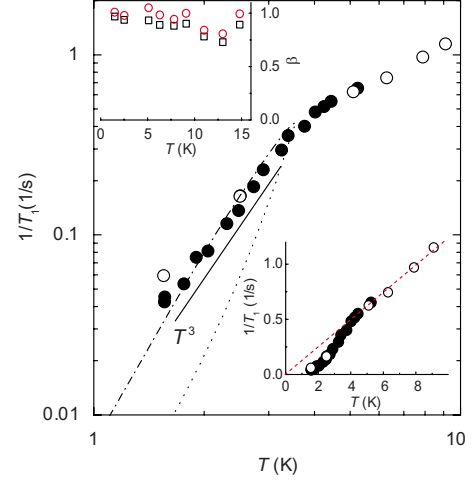


FIG. 5. (Color online) Log plot of ^{13}C $1/T_1$ at 0.4 GPa at $H_0 = 2.0$ T (closed circle) and 3.5 T (open circles) applied parallel to the conducting layer. Broken and dotted lines are calculated results for $\Delta/T_c = 2.2$ and 4.0 in the d -wave pairing. Lower inset: a linear plot of $1/T_1$. Upper inset: the exponent β of the stretched exponential fit to the recovery curve at 3.5 T. Circles and squares are obtained for A1 and all ^{13}C lines.

begins to decrease more steeply below T_c of 3.5 K. A coherence peak just below T_c , which would indicate a full-gap superconductor, is not corroborated within the current experimental resolution. Instead, T^3 behavior is seen below T_c down to 1.5 K. The $1/T_1$ behavior is consistent with a non- s -wave anisotropic superconducting gap with line nodes. This feature, the T^3 dependence persisting up to T_c , was also observed in CeIrIn $_5$ (Ref. 36) and (TMTSF) $_2$ ClO $_4$ (Ref. 37), while $1/T_1$ of κ -(ET) $_2$ Cu[N(CN) $_2$]Br (Refs. 5 and 38) and YBa $_2$ Cu $_3$ O $_7$ had a steep drop just below T_c . The difference may be attributed to the superconducting coupling strength, $\Delta/k_B T_c$, where Δ and k_B denote the superconducting order parameter and the Boltzmann constant, respectively. Assuming d -wave pairing, for example, the present data are close to the calculations for $\Delta/k_B T_c = 2.2$, while $\Delta/k_B T_c = 4.0$ gives a sharp drop in $1/T_1$ near T_c and T^3 behavior for $T/T_c < 0.5$.⁴

IV. CONCLUSION

We reported ^{13}C NMR investigations of the Mott transition and superconducting state in κ -(ET) $_2$ Cu $_2$ (CN) $_3$ under pressure, which is at ambient pressure the spin-liquid Mott insulator with a half-filled triangular lattice. The Mott transition from the spin-liquid state to the Fermi-liquid state was accompanied by a strong suppression of the dynamical spin susceptibility probed by the nuclear-spin-lattice relaxation rate, but the static spin susceptibility was less affected, and maintained a high value above the superconducting transition temperature. The Fermi-liquid metallic state followed Pauli paramagnetic behavior and Korringa's law, without opening a pseudogap, unlike the metallic phase neighboring the antiferromagnetic insulator. In the superconducting state, the nuclear-spin-lattice relaxation rate followed a T^3 dependence, as expected for a nodal order parameter. The finite

decrease in spin susceptibility below T_c may indicate spin-singlet Cooper pairing. While the possibility of mixed triplet pairing is intriguing, a possible extrinsic effect due to rf heating should be ruled out by further experiments.

ACKNOWLEDGMENTS

We thank A. Kawamoto for synthesis of ^{13}C -substituted

ET, and P. A. Lee and T. Senthil for valuable discussions. This work was partially supported by Grants-in-Aid for Scientific Research in the Priority Area (Grant No. 17071003) and Innovative Area (Grant No. 20110002) from the MEXT, Grants-in-Aid for Scientific Research (A) (Grant No. 20244055) and (C) (Grant No. 20540346) from the JSPS, and by Global COE Program: Global Center of Excellence for the Physical Sciences Frontier (No. G04).

*Present address: Institute for Advanced Research, Nagoya University, Japan.

†Present address: Meijo University, Nagoya, Japan.

- ¹P. A. Lee, N. Nagaosa, and X.-G. Wen, *Rev. Mod. Phys.* **78**, 17 (2006).
- ²F. Steglich, *J. Phys. Soc. Jpn.* **74**, 167 (2005).
- ³P. W. Anderson, *Mater. Res. Bull.* **8**, 153 (1973).
- ⁴M. Sigrist and K. Ueda, *Rev. Mod. Phys.* **63**, 239 (1991).
- ⁵K. Kanoda, *Physica C* **282-287**, 299 (1997); *Hyperfine Interact.* **104**, 235 (1997); *J. Phys. Soc. Jpn.* **75**, 051007 (2006).
- ⁶B. J. Powell and R. H. McKenzie, *Phys. Rev. B* **69**, 024519 (2004).
- ⁷K. Miyagawa, A. Kawamoto, and K. Kanoda, *Phys. Rev. Lett.* **89**, 017003 (2002).
- ⁸Y. Shimizu, K. Miyagawa, K. Kanoda, M. Maesato, and G. Saito, *Phys. Rev. Lett.* **91**, 107001 (2003).
- ⁹Y. Shimizu, K. Miyagawa, K. Kanoda, M. Maesato, and G. Saito, *Phys. Rev. B* **73**, 140407(R) (2006).
- ¹⁰S. Yamashita, Y. Nakazawa, M. Oguni, Y. Oshima, H. Nojiri, Y. Shimizu, K. Miyagawa, and K. Kanoda, *Nat. Phys.* **4**, 459 (2008).
- ¹¹M. Yamashita, N. Nakata, Y. Kasahara, T. Sasaki, N. Yoneyama, N. Kobayashi, S. Fujimoto, T. Shibauchi, and Y. Matsuda, *Nat. Phys.* **5**, 44 (2009).
- ¹²P. A. Lee, *Science* **321**, 1306 (2008).
- ¹³O. I. Motrunich, *Phys. Rev. B* **72**, 045105 (2005).
- ¹⁴F. Becca, L. Capriotti, A. Parola, and S. Sorella, *Phys. Rev. B* **76**, 060401(R) (2007).
- ¹⁵S. S. Lee, *Phys. Rev. B* **78**, 085129 (2008).
- ¹⁶Y. Qi, C. Xu, and S. Sachdev, *Phys. Rev. Lett.* **102**, 176401 (2009).
- ¹⁷Y. Kurosaki, Y. Shimizu, K. Miyagawa, K. Kanoda, and G. Saito, *Phys. Rev. Lett.* **95**, 177001 (2005).
- ¹⁸S. Lefebvre, P. Wzietek, S. Brown, C. Bourbonnais, D. Jerome, C. Meziere, M. Fourmigue, and P. Batail, *Phys. Rev. Lett.* **85**, 5420 (2000).
- ¹⁹H. Kondo and T. Moriya, *J. Phys. Soc. Jpn.* **73**, 812 (2004).
- ²⁰T. Watanabe, H. Yokoyama, M. Ogata, Y. Tanaka, and J. Inoue, *J. Phys. Soc. Jpn.* **75**, 074707 (2006).
- ²¹R. T. Clay, H. Li, and S. Mazumdar, *Phys. Rev. Lett.* **101**, 166403 (2008).
- ²²J. Schmalian, *Phys. Rev. Lett.* **81**, 4232 (1998).
- ²³B. Kyung and A.-M. S. Tremblay, *Phys. Rev. Lett.* **97**, 046402 (2006).
- ²⁴B. J. Powell and R. H. McKenzie, *Phys. Rev. Lett.* **94**, 047004 (2005); **98**, 027005 (2007).
- ²⁵H. X. Huang, Y. Q. Li, J. Y. Gan, Y. Chen, and F. C. Zhang, *Phys. Rev. B* **75**, 184523 (2007).
- ²⁶P. Sahebsara and D. Senechal, *Phys. Rev. Lett.* **97**, 257004 (2006).
- ²⁷J. Y. Gan, Y. Chen, and F. C. Zhang, *Phys. Rev. B* **74**, 094515 (2006).
- ²⁸P. Wrobel and W. Suleja, *Phys. Rev. B* **76**, 214509 (2007).
- ²⁹S.-S. Lee, P. A. Lee, and T. Senthil, *Phys. Rev. Lett.* **98**, 067006 (2007).
- ³⁰V. Galitski and Y. B. Kim, *Phys. Rev. Lett.* **99**, 266403 (2007).
- ³¹K. Miyagawa, K. Kanoda, and A. Kawamoto, *Chem. Rev.* **104**, 5635 (2004).
- ³²J. Larsen and C. Lenoir, *Synthesis* **1989**, 134 (1989).
- ³³P. A. Mansky, P. M. Chaikin, and R. C. Haddon, *Phys. Rev. Lett.* **70**, 1323 (1993).
- ³⁴S. M. De Soto, C. P. Slichter, H. H. Wang, U. Geiser, and J. M. Williams, *Phys. Rev. Lett.* **70**, 2956 (1993).
- ³⁵M. Rahal, D. Chasseau, J. Gaultier, L. Ducasse, M. Kurmoo, and P. Day, *Acta Crystallogr., Sect. B: Struct. Sci.* **53**, 159 (1997).
- ³⁶G.-q. Zheng, K. Tanabe, T. Mito, S. Kawasaki, Y. Kitaoka, D. Aoki, Y. Haga, and Y. Onuki, *Phys. Rev. Lett.* **86**, 4664 (2001).
- ³⁷M. Takigawa, H. Yasuoka, and G. Saito, *J. Phys. Soc. Jpn.* **56**, 873 (1987).
- ³⁸H. Mayaffre, P. Wzietek, D. Jérôme, C. Lenoir, and P. Batail, *Phys. Rev. Lett.* **75**, 4122 (1995).